Biointerface Research in Applied Chemistry
Platinum Open Access Journal (ISSN: 2069-5837)

Article
Volume 12, Issue 2, 2022, 1628 - 1637
https://doi.org/10.33263/BRIAC122.16281637

Photo-Inactivation *Staphylococcus aureus* by Using Formulation of Mn-N-TiO_2 Composite Coated Wall Paint

Maulidiyah Maulidiyah [1], Prima Endang Susilowati [1], Nur Khalimatussa'diyah Mudhafar [1], La Ode Agus Salim [1], Dwiprayogo Wibowo [2], Muhammad Zakir Muzakkar [1], Irwan Irwan [1], Zul Arham [3], Muhammad Nurdin [1,*]

1 Department of Chemistry, Faculty of Mathematics and Natural Sciences, Universitas Halu Oleo, Jl. HEA Mokodompit Kampus Baru, Kendari 93232 – Southeast Sulawesi, Indonesia
2 Department of Environmental Engineering, Faculty Engineering, Universitas Muhammadiyah Kendari, Kendari 93117 – Southeast Sulawesi, Indonesia
3 Department of Mathematics and Natural Science, Institut Agama Islam Negeri Kendari, Kendari 93116 – Southeast Sulawesi, Indonesia
* Correspondence: mnurdin06@yahoo.com (M.N.);

Scopus Author ID 56678695400

Received: 27.04.2021; Revised: 25.05.2021; Accepted: 29.05.2021; Published: 9.06.2021

Abstract: Photo-inactivation *Staphylococcus aureus* bacteria based on Mn-N-TiO_2 composite coated wall paint is a unique study for preparing antibacterial material applied on wall house. Utilization of mixed material plays a role in activating under visible light illumination by sunlight to inactivate bacterially. Preparation of Mn-N-TiO_2 composite by the sol-gel method using reflux for 3 h and coated with wall paint. The bacterial test uses Nutrient Broth (NB) to grow S. aureus, which is tested 3 times (triple). The yellow sol-gel produced by TiO_2 doped Mn and N is functionally decreased bandgap as 2.8 eV. Subsequently, SEM/EDX data has characterized that the Ti, O, C, N and Mn elements are identified from composite Meanwhile, Ca is material produced from $CaCO_3$ as wall paint colloidal. Based on these results, we report that the high concentration of Mn-N-TiO_2 composite exhibited that the high inactivation response of *S. aureus* bacteria with 60% concentration is 87.73%.

Keywords: TiO_2; wall paint; *S.aureus*; photo-inactivation; bacterial.

1. Introduction

The utilization of wall paint has generally been used to obtain the beauty house the shape of color and shiny [1]. In addition, it is protecting sunlight irradiation, weather, dust, lichen, and leak [2]. These conditions also attached bacteria and lichen, which is difficult for cleaning, caused moistly and not protected by wall paint [3,4]. Needed attention for repairing walls by using self-cleaning utilize smart material which has the substance's ability to clean themselves from dirt through chemical reactions. By this technology, it is expected to be able to maintain the aesthetic value of the walls [5].

In the last decades, self-cleaning applications have been developed in wall paint by using a photocatalyst based on titanium dioxide (TiO_2) nanoparticles [6]. Photocatalysis paint contained photoactive TiO_2 as a white pigment that effectively removed organic pollutants, inorganic, impurities substances, microbes, and stains [7–9]. It is a chemical reaction process by energy photons from ultraviolet (UV) irradiation [10]. The effect of TiO_2 photocatalyst can decompose organic compounds into CO_2 and H_2O, which is applied to decompose impurities and microbes attached to the wall's surface [11,12]. In addition, the unique properties of TiO_2

photocatalyst are most successful as self-cleaning such as glass, marble [13], lime [14], cement [15], copper [16] etc.

TiO_2 photocatalyst is a semiconductor material widely used for optoelectronic, microelectronics, sensor, anti-fog, self-cleaning, water cleaning, and inactivation of the microorganism [17–20]. However, the TiO_2 photocatalyst only active under UV light illumination caused the high bandgap energy (Eg) of 3.2 eV anatase phase, thus limited to high performance under sunlight radiation [21–23]. The application of TiO_2 photocatalyst in wall paint very suitable for self-cleaning as resin/binder in the wall paint mixture, white pigment, and antimicrobial material [24,25]. Needed decorated TiO_2 photocatalyst by metal or non-metal dopants decreases bandgap energy (optical properties) as applied under visible illumination [26].

The modern strategy to optimize the performance of TiO_2 photocatalyst under visible region by doping method using metal or non-metal atoms on the TiO_2 crystal matrix. The metal-doped such as Iron (Fe), Cobalt (Co), Nickel (Ni), Cupprum (Cu), and Manganese (Mn) has been studied to increase the optical properties in the conduction band (Cb) as the role of trapping electron excited in Cb as a p-type semiconductor [27]. The Mn metal is one of the transition metals that is electropositive and has good electrical conductivity usefully as a dopant in TiO_2 photocatalyst [28,29]. Meanwhile, the doping of non-metal like Carbon (C) [30], Sulfur (S) [31], Fluorine (F) [32], Phosphor (P) [33], and Nitrogen (N) [34] was proven as an n-type semiconductor which is effectively shifting the optical absorption of TiO_2 photocatalyst under the lowest energy level [35]. The couple doped (co-doped) was increased the stability of electron in semiconductor, high-response ability, and high-optical properties. This research explores the co-doped of Mn, N co-doped TiO_2 photocatalyst then coated in wall paint, which is a high self-cleaning property for antibacterial activity. The *S. aureus* has selected due to the gram-positive bacterial group that is resulting in skin disorders when human has contact with material containing this bacteria. This research explores the co-doped Mn, N co-doped TiO_2 photocatalyst, then coated in wall paint with high self-cleaning properties for antibacterial activity. The *S. aureus* has been selected due to the gram-positive bacterial group resulting in skin disorders of human contact.

2. Experimental Methods

2.1 Preparation of Mn-N-TiO_2 composite.

Synthesis of Mn-N-TiO_2 composite was conducted by mixing of 15 mL EtOH, 2.0 mL Aquades, 1.0 mL Acetic Acid (0.5 M) into a reflux flask which is containing 4.0 mL of Titanium tetra- isopropoxide (TTIP), 0.5 mL Acetyl Acetonate (AcAc) and 15 mL EtOH. Subsequently, it was stirred by using a magnetic stirrer for 1.0 h at a temperature of 50°C and followed by the addition of 2 mL 0.5 M $CO(NH_2)_2$ as Nitrogen source and 1.0 mL 2.5% Mn solution to obtain Mn and N sol-gel TiO_2 composite. It evaporates at room temperature for 48 h to form a gel and is heated at 80°C for 30 min. To obtain the Mn-N-TiO_2 powder, we calcinated the sol-gel Mn-N-TiO_2 composite at a temperature of 400°C for 1 h and characterized by UV-Vis Diffuse Reflectance Spectroscopy (UV-DRS) to observe optical properties.

2.3 Preparation of Mn-N-TiO_2 composite coated in wall paint colloidal.

The solution test of Mn-N-TiO_2 composite was prepared by a variation of 40%, 50%, and 60% diluted by distilled water in 10 mL and stirring at 50°C for 2 h. It was mixed with 20 mL polyethylene glycol (PEG) as coagulate material to be easily integrated with wall paint material and stirring at 60°C for 15 min. Mn-N-TiO_2/PEG was mixed for 30 min with 250-gram wall paint colloidal. Finally, it was characterized by Scanning electron microscopy with energy-dispersive X-ray spectroscopy (SEM/EDX) to obtain the morphology characteristic and elements on the surface.

2.3 Antibacterial activity test.

The antibacterial activity test was carried out using cement as adhesive walls house containing with variation concentration of Mn-N-TiO_2 coated wall paint. Thus, it was dried and added into 15 mL NB, which has planted with 100 µL *S. aureus* bacteria (0.5 Mc). Subsequently, it was stored at room temperature for 7 days under visible light illumination and dipped into 20 mL *saline* solution. It is diluted as the concentration of 10^0, 10^{-1}, 10^{-2}, 10^{-3} and taken as 100 µL then mixed in Nutrient Agar (NA) were inserted into a petri dish. We test antibacterial properties into Mn-N-TiO_2 composite coated wall paint by variating concentration. The total colony of bacteria was observed by the instrument total plate count (TPC) to obtain the inactivation *S. aureus* bacteria percentage.

3. Results and Discussion

3.1 Preparation of Mn-N-TiO_2 composite.

Preparation of Mn-N-TiO_2 composite has been conducted using a sol-gel method that is useful for TiO_2 nanoparticle synthesized doped metal and non-metal. This method was advantageous for controlling pH stability, temperature, and rate hydrolysis [36]. The sol-gel method can make a nano-sized particle, uniform size, not lumpy, pure and homogeneous [37–39]. In addition, the parameters are varied, the size and the distribution of pore can be controlled and relatively inexpensive and easy to apply [11].

In this study, we use the alkoxide source as a precursor of TTIP, which serves as a distribution medium for dopant ions to form the Mn-N-TiO_2 composite. This method has been applied by Nurdin *et al.*. that the organic solvent has a role for preserve titanium stability in order to protect the oxidation reaction [40]. The addition of AcAc is a ligand chelate titanium metal and to form mesostructure-assisted TiO_2 anatase. While, ethanol solvent to control the rate of hydrolysis due to the TTIP is very easy to transform into $Ti(OH)_4$ if it reacts by water. These solvents were refluxed at 50°C for 3 h to increase interaction and homogeneity particle. Subsequently, $MnCl_2.4H_2O$ as Mn metal and $CO(NH_2)_2$ as Nitrogen sources have been added into sol TiO_2, stirring for 0.5 h to form an Mn-N-TiO_2 composite. Finally, the sol Mn-N-TiO_2 was evaporated for 24 h to obtain the sol-gel (Figure 1a).

Sol-gel has been produced with a yellow color that plays a role in absorbing the visible region if it illuminates by visible light and responds to the excitation electron in the conduction band. This phenomenon due to the range space band gap has decreased after adding the Mn metal (electron trapping) while the N non-metal distributing hole for high oxidation is initiated to degrade or inactivate bacteria.

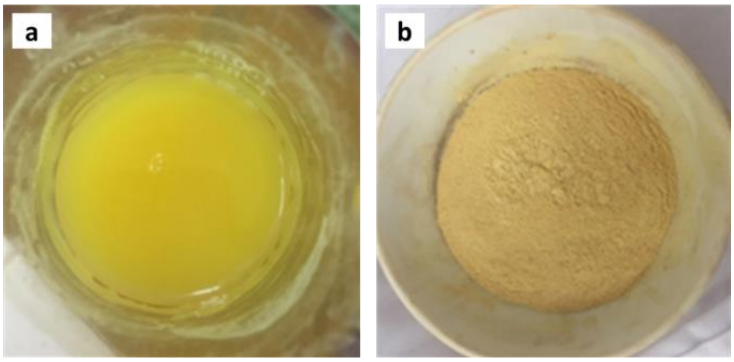

Figure 1. (**a**) Sol-gel Mn-N-TiO_2 composite; (**b**) Powder of Mn-N-TiO_2 composite.

Effectiveness preparation of Mn-N-TiO_2 composite, we calcination to obtain the Mn-N-TiO_2 composite powder because of anatase crystal has photoactive properties with high surface area. It has calcinated at 500°C for 1 h to release solvents and also high crystallinity reconstructure produced as powder of Mn-N-TiO_2 composite. In addition, the high temperature is very useful for preparing TiO_2 nanocomposite due to the collision of atoms to obtain the small particle (Figure 1b) [41].

3.2 Characterization of Mn-N-TiO_2 composite.

3.2.1 UV-Vis diffuse reflectance spectroscopy.

Bandgap energy has been analyzed to observe optical properties by using diffuse reflectance spectroscopy **(**UV-Vis DRS). It was employed to examine the optical response of the starting material TiO_2, we have compared the TiO_2 anatase with Mn-N-TiO_2 composite for effectiveness doped metal and non-metal The bandgap is significantly affected by factors such as phase structure, temperature and crystal size [42,43]. Figure 2 shows that the bandgap energy of sol-gel TiO_2 after calcination of 3.27 eV. Its same result by Zhang *et al.* [44] the fabrication of TiO_2 by dip-coating technique resulting in the anatase crystal structure. TiO_2 anatase bandgap of 3.2 eV has a response under UV region 388 nm, which cannot apply under sunlight irradiation. The Mn-N-TiO_2 composite is also characterized to discover bandgap energy decreases caused effect of Mn and N as dopants. Figure 2 the Mn metal and N non-metal doped TiO_2 composite has successfully decreased bandgap energy with a value of 2.8 eV.

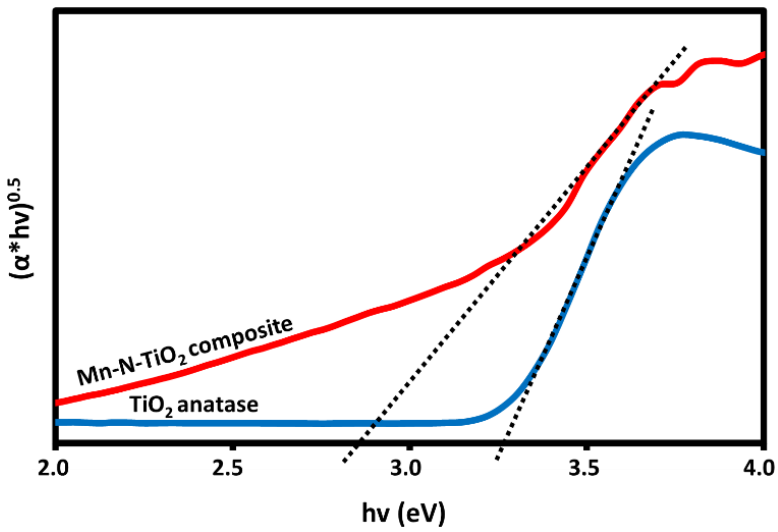

Figure 2. Bandgap spectra of TiO_2 compared with Mn-N-TiO_2 composite.

3.2.2. Scanning electron microscopy with energy-dispersive X-ray spectroscopy.

The characterization morphology of Mn-N-TiO_2 coated on wall paint has been carried out by using scanning electron microscopy with energy-dispersive X-ray spectroscopy (SEM/EDX) showed that the morphology deepest cracks between contacted particulate particles. The temperature effect has formed a crystallinity of particles with particle variation size. We conclude that the white particles exhibited TiO_2 material because TiO_2 atoms have high-density and molecular weight, reflecting more electrons that appear brighter than low-density atoms. Figure 3 has examined the average particle size of Mn-N-TiO_2 coated on wall paint was 2.075 μm. Meanwhile, the wall paint contained other elements such as CaCO3, binders, and others covered in TiO_2 crystals.

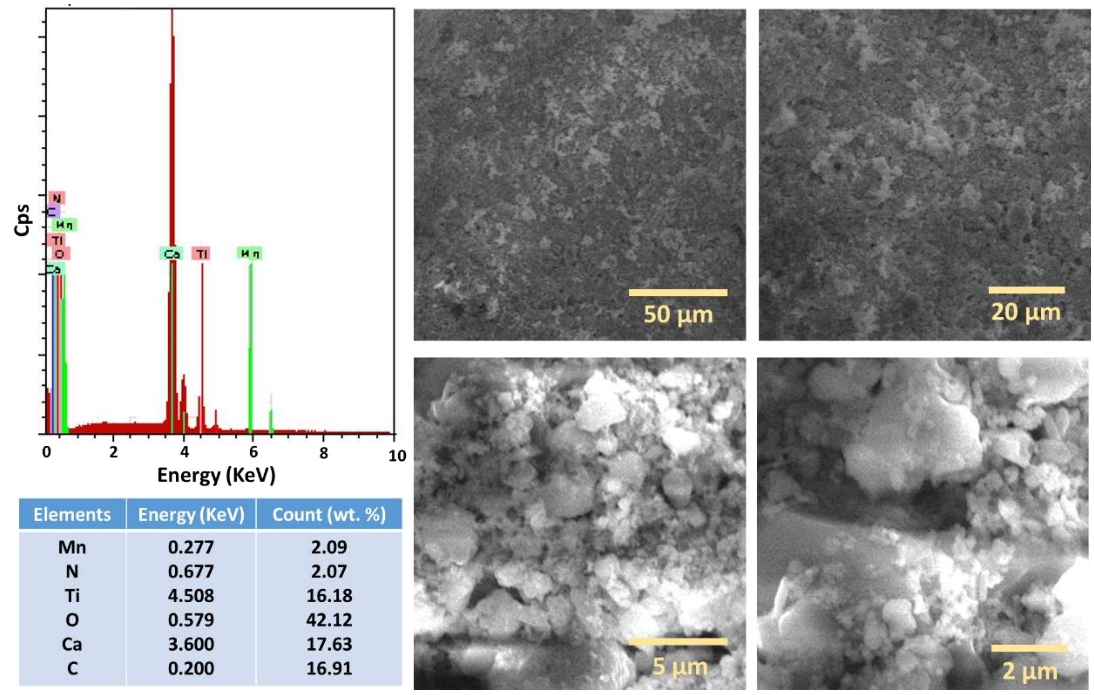

Elements	Energy (KeV)	Count (wt. %)
Mn	0.277	2.09
N	0.677	2.07
Ti	4.508	16.18
O	0.579	42.12
Ca	3.600	17.63
C	0.200	16.91

Figure 3. Morphology and elements characterization of Mn-N-TiO_2 composite coated on wall paint

We observe by using EDX data of Mn-N-TiO_2 composite coated on wall painting shows that the Ca atoms have high peaks due to $CaCO_3$ is a wall paint composition source. Based on Figure 3 exhibits that the Mn peak was obtained at 0.277 KeV; N at 0.677 KeV; Ti at 4.508 KeV, and O at 0. The presence of Mn and N peaks indicated that doping between Mn (metal) and N (non-metal) were successful. In addition, the presence of Ca characterized on 3.75 KeV. These results had been compared with Paul and Choudhury and Gurkan *et al.*., reporting that Ca and C can be derived from the main raw material of paint composers $CaCO_3$ as emulsion paints [45,46]. By EDX data, we obtain the content of the mixer element of Mn-N-TiO_2 composite coated on wall paint (Figure 3).

3.3. Antibacterial activity test of Mn-N-TiO_2 composite coated wall paint.

The potency of Mn-N-TiO_2 composite-wall paint as antibacterial activity was conducted under visible light illumination. Bacterial testing was carried out quantitatively based on the percentage reduction of bacterial colonies on media. *S. aureus* was used for testing the ability sample because this bacteria is generated nosocomial infections such as pneumonia, mastitis, phlebitis, meningitis, urinary tract infections, osteomyelitis and endocarditis.

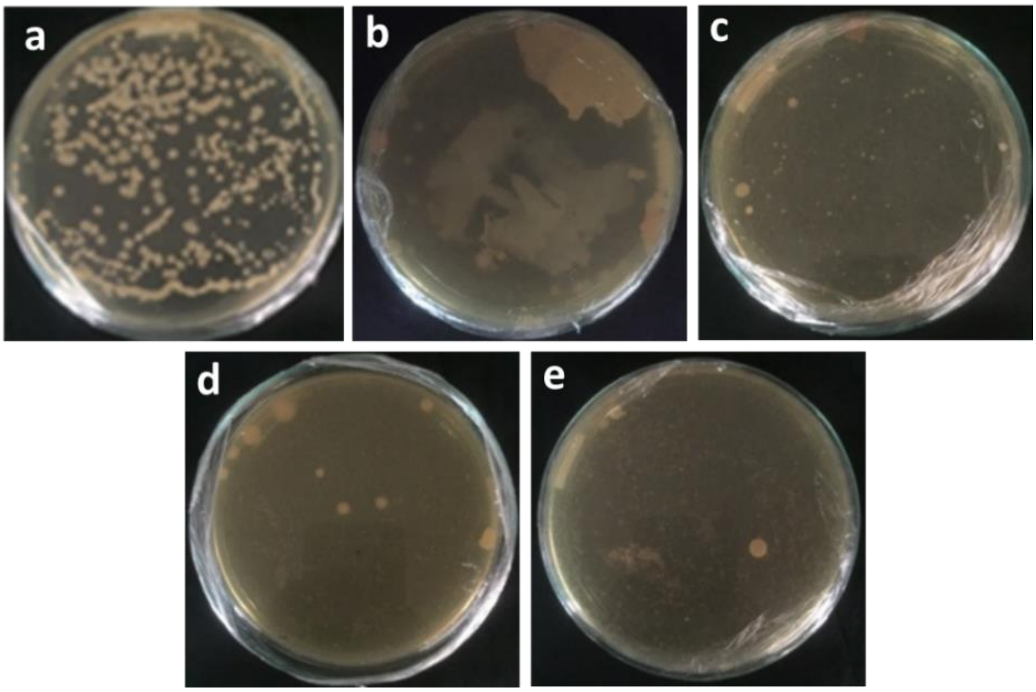

Figure 4. Photo-inactivation of *S. aureus* by variation treatment, (**a**) Without wall paint; (**b**) wall paint; (**c**) Wall paint coated Mn-N-TiO_2 composite (40%); (**d**) Wall paint coated Mn-N-TiO_2 composite (50%); (**e**) Wall paint coated Mn-N-TiO_2 composite (60%).

Variation concentration of Mn-N-TiO_2 composite that was added into the wall paint to obtain the high antibacterial activity test with variation 40%, 50%, and 60%. These variations had been repetitions by a triple to produce more concrete and accurate data (Table 1). The antibacterial activity test of Mn-N-TiO_2 composite variations to inhibit *S. aureus* can be seen in Figure 4 and Figure 5.

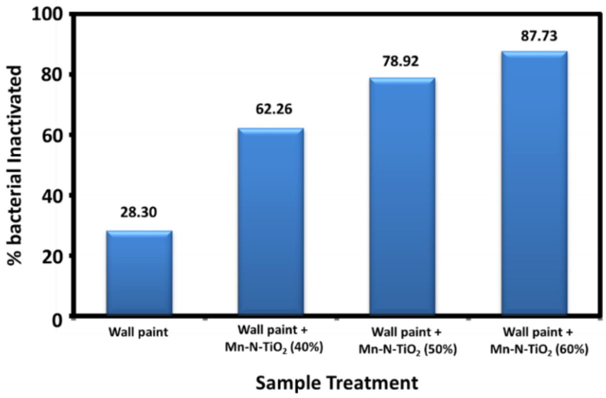

Figure 5. Percentage of inhibiting *S. aureus* bacterial using Mn-N-TiO_2 composite coated wall paint

Table 1. Inhibition *S. aureus* bacterial using Mn-N-TiO_2 composite coated wall paint (Triplo).

Sample	Treatment			Negative control			Total of Colony		
	Nutrient Broth + S. Aureus			Nutrient Broth without S. aureus					
	1	2	3	1	2	3	1	2	3
Without wall paint	208×10^3	141×10^3	1×10^3	63×10^3	35×10^3	137×10^3	145×10^3	106×10^3	99×10^3
Wall paint	109×10^3	222×10^3	198×10^3	23×10^3	130×10^3	135×10^3	86×10^3	92×10^3	73×10^3
Wall paint + Mn-N-TiO_2 (40%)	41×10^3	78×10^3	158×10^3	12×10^3	21×10^3	107×10^3	29×10^3	57×10^3	51×10^3
Wall paint + Mn-N-TiO_2 (50%)	9×10^3	35×10^3	106×10^3	3×10^3	21×10^3	58×10^3	6×10^3	14×10^3	48×10^3
Wall paint + Mn-N-TiO_2 (60%)	3×10^3	14×10^3	34×10^3	2×10^3	3×10^3	3×10^3	1×10^3	11×10^3	31×10^3

Antibacterial activity test has been carried out using Mn-N-TiO_2 composite coated wall paint to inhibit the *S. aureus* bacteria. The presence of several bacterial colonies formed above the nutrient agar surface. In addition, the Mn-N-TiO_2 concentration variation also affected the total bacterial colonies. Based on data, the Mn-N-TiO_2 concentration of 60% coated wall paint has better activity in inactivating S. aureus bacteria under visible illumination. This due to Mn-N-TiO_2 initiated OH radical formed that capable of reaction bacterial. Reactive radical species (ROS) consisting of • OH and • O_2^- are produced from photogeneration processes on the titania surface by strong oxidative substances to attack cell walls and cell membranes in bacteria.

Inactivated bacterial cells by photocatalysis will decrease permeability cells. Mechanism to inactivate bacterial cell, first the contacting on cell walls by an oxidation process namely of lysis process. Subsequently, oxidation reaction on the cytoplasm membrane decreases the permeability cell and then the metabolism cell will defunct. The Mn-N-TiO_2 composite coated wall paint can also reach damaged cell membranes and direct attacks can accelerate cell death. We discover that the wall paint is also developed for antibacterial properties and utilized on wall homes or hospitals that are protecting S. aureus. In addition, Mn-N-TiO_2 composite has more advantages in the photocatalyst system such as wideband, photostable, inert, and is able to degrade organic compounds into CO_2 and H_2O, which are relatively harmless.

4. Conclusions

Preparation of Mn-N-TiO_2 composite coated on wall paint has been decreased bandgap energy of TiO_2 with 2.8 eV, which is active under visible illumination. The microstructure has been observed that particles' average morphology size is 2.075 µm with percentage composition unsure of Mn at 2.09%, N of 2.07%, Ti of 22.18%, O of 52.12%. In addition, wall paint has contained $CaCO_3$ with a percentage mass of Ca is 18.63% and C of 2.91%. The potency of Mn-N-TiO_2 composite in inactivating *S. aureus*.

Funding

This research was funded by the Ministry of Research and Technology/ National Research and Innovation Agency (KEMRISTEK/BRIN), the Republic of Indonesia, as a part of the Applied Research Award 2021 Grant No. 270/SP2H/LT/DRPM/2021.

Acknowledgments

We acknowledge the Titania Research Group and laboratory facilities support from the Department of Chemistry, Universitas Halu Oleo, Kendari, Indonesia.

Conflicts of Interest

We declare that this article has no conflict of interest

References

1. Bal, S.; Sanli, N.O. Evaluation of the effectiveness of antibacterial wall paint to enhance the hygienic conditions of the interiors. *J. Fac. Eng. Archit. Gazi Univ.* **2020**, *35*, 1913-1922.
2. Gandolfo, A.; Bartolomei, V.; Truffier-Boutry, D.; Temime-Roussel, B.; Brochard, G.; Bergé, V.; Wortham, H.; Gligorovski, S. The impact of photocatalytic paint porosity on indoor NOx and HONO levels. *Phys. Chem. Chem. Phys.* **2020**, *22*, 589–598, https://doi.org/10.1039/C9CP05477D.
3. Karlsson, M.C.F.; Abbas, Z.; Bordes, R.; Cao, Y.; Larsson, A.; Taylor, P.; Steenari, B.-M. Characterisation

of silicon, zirconium and aluminium coated titanium dioxide pigments recovered from paint waste. *Dye. Pigment.* **2019**, *162*, 145–152, https://doi.org/10.1016/j.dyepig.2018.06.028.
4. Maulidiyah, M.; Darmawan, A.; Hasan, A.; Wibowo, D.; Salim, L.O.A.; Ansharullah, A.; Mustapa, F.; Nurdin, I.F.A.; Nurdin, M. Isolation, structure elucidation, and antidiabetic test of vicanicin compound from lichen *Teloschistes flavicans*. *J. Appl. Pharm. Sci.* **2020**, *10*, 001-009, https://doi.org/10.7324/JAPS.2020.10111.
5. Děkanovský, L.; Elashnikov, R.; Kubiková, M.; Vokatá, B.; Švorčík, V.; Lyutakov, O. Dual-Action flexible antimicrobial material: switchable self-cleaning, antifouling, and smart drug release. *Adv. Funct. Mater.* **2019**, *29*, 1901880, https://doi.org/10.1002/adfm.201901880.
6. Wojciechowski, K.; Gutarowicz, M.; Janke, K.; Jurek, I.; Kaczorowski, M.; Mierzejewska, J.; Parzuchowski, P. Colloidal Stability of Positively Charged Dispersions of Styrene and Acrylic Copolymers in the Presence of TiO_2 and $CaCO_3$. *Colloids and Interfaces*, **2019**, *3*, https://doi.org/10.3390/colloids3010020.
7. Peeters, H.; Keulemans, M.; Nuyts, G.; Vanmeert, F.; Li, C.; Minjauw, M.; Detavernier, C.; Bals, S.; Lenaerts, S.; Verbruggen, S.W. Plasmonic gold-embedded TiO_2 thin films as photocatalytic self-cleaning coatings. *Appl. Catal. B Environ.* **2020**, *267*, 118654, https://doi.org/10.1016/j.apcatb.2020.118654.
8. Killivalavan, A.; Prabakar, A.C.; Chandra Babu, K.; Naidu, B.; Sathyaseelan, G.; Rameshkumar, D.; Sivakumar, K.; Senthilnathan, I.; Baskaran, E.; Manikandan, B.R.R. Synthesis and characterization of pure and Cu doped CeO_2 nanoparticles: photocatalytic and antibacterial activities evaluation. *Biointerface Res. Appl. Chem* **2020**, *10*, 5306–5311, https://doi.org/10.33263/BRIAC102.306311.
9. Khanmohammadi, S.; Karimian, R.; Hajibonabi, F.; Mostafidi, E.; Tanomand, A.; Edjlali, L.; Azami, Z.K.; Mehrabani, M.G.; Kafil, H.S. Polythiophene/TiO_2 and polythiophene/ZrO_2 nanocomposites: Physical and antimicrobial properties against common infections. *Biointerface Res. Appl. Chem.* **2018**, *8*, 3457–3462.
10. Al-Mamun, M.R.; Kader, S.; Islam, M.S.; Khan, M.Z.H. Photocatalytic activity improvement and application of UV-TiO_2 photocatalysis in textile wastewater treatment: A review. *J. Environ. Chem. Eng.* **2019**, *7*, 103248, https://doi.org/10.1016/j.jece.2019.103248.
11. Maulidiyah, M.; Azis, T.; Nurwahidah, A.T.; Wibowo, D.; Nurdin, M. Photoelectrocatalyst of Fe co-doped N-TiO_2/Ti nanotubes: Pesticide degradation of thiamethoxam under UV–visible lights. *Environ. Nanotechnology, Monit. Manag.* **2017**, *8*, 103–111, https://doi.org/10.1016/j.enmm.2017.06.002.
12. Nurdin, M.; Maulidiyah, M.; Salim, L.O.A.; Muzakkar, M.Z.; Umar, A.A. High performance cypermethrin pesticide detection using anatase TiO_2-carbon paste nanocomposites electrode. *Microchem. J.* **2019**, *145*, https://doi.org/10.1016/j.microc.2018.11.050.
13. Kapridaki, C.; Maravelaki-Kalaitzaki, P. TiO_2–SiO_2–PDMS nanocomposite hydrophobic coating with self-cleaning properties for marble protection. *Prog. Org. Coatings* **2013**, *76*, 400–410, https://doi.org/10.1016/j.porgcoat.2012.10.006.
14. Munafò, P.; Quagliarini, E.; Goffredo, G.B.; Bondioli, F.; Licciulli, A. Durability of nano-engineered TiO_2 self-cleaning treatments on limestone. *Constr. Build. Mater.* **2014**, *65*, 218–231, https://doi.org/10.1016/j.conbuidmat.2014.04.112.
15. Jimenez-Relinque, E.; Rodriguez-Garcia, J.R.; Castillo, A.; Castellote, M. Characteristics and efficiency of photocatalytic cementitious materials: Type of binder, roughness and microstructure. *Cem. Concr. Res.* **2015**, *71*, 124–131, https://doi.org/10.1016/j.cemconres.2015.02.003.
16. Qing, Y.; Yang, C.; Sun, Y.; Zheng, Y.; Wang, X.; Shang, Y.; Wang, L.; Liu, C. Facile fabrication of superhydrophobic surfaces with corrosion resistance by nanocomposite coating of TiO_2 and polydimethylsiloxane. *Colloids Surfaces A Physicochem. Eng. Asp.* **2015**, *484*, 471–477, https://doi.org/10.1021/am501539b.
17. Natsir, M.; Putri, Y.I.; Wibowo, D.; Maulidiyah, M.; Salim, L.O.A.; Azis, T.; Bijang, C.M.; Mustapa, F.; Irwan, I.; Arham, Z.; Nurdin, M. Effects of Ni–TiO_2 pillared Clay–Montmorillonite composites for photocatalytic enhancement against reactive orange under visible light. *J. Inorg. Organomet. Polym. Mater*. **2021**, 1-11, https://doi.org/10.1007/s10904-021-01980-9.
18. Nurdin, M.; Dali, N.; Irwan, I.; Maulidiyah, M.; Arham, Z.; Ruslan, R.; Hamzah, B.; Sarjuna, S.; Wibowo, D. Selectivity Determination of Pb^{2+} Ion based on TiO_2-Ionophores BEK6 as carbon paste electrode composite. *Anal. Bioanal. Electrochem.* **2018**, *10*, 1538–1547.
19. Dzinun, H.; Othman, M.H.D.; Ismail, A.F.; Puteh, M.H.; Rahman, M.A.; Jaafar, J. Photocatalytic degradation of nonylphenol by immobilized TiO_2 in dual layer hollow fibre membranes. *Chem. Eng. J.* **2015**, *269*, 255–261, https://doi.org/10.1016/j.cej.2015.01.114.
20. Nurdin, M.; Arham, Z.; Rasyid, J.; Maulidiyah, M.; Mustapa, F.; Sosidi, H.; Ruslan, R.; Salim, L.O.A. Electrochemical performance of carbon paste electrode modified TiO_2/Ag-Li (CPE-TiO_2/Ag-Li) in determining fipronil compound. *J. Phys. Conf. Ser.* **2021**, *1763*, 012067, https://doi.org/10.1088/1742-6596/1763/1/012067.
21. Li, G.; Fang, K.; Ou, Y.; Yuan, W.; Yang, H.; Zhang, Z.; Wang, Y. Surface study of the reconstructed anatase TiO_2 (001) surface. *Prog. Nat. Sci. Mater. Int.* **2021**, *31*, 1-13, https://doi.org/10.1016/j.pnsc.2020.11.002.
22. Liu, X.; Fu, J. Electronic and elastic properties of the tetragonal anatase TiO_2 structure from first principle calculation. *Optik (Stuttg)* **2020**, https://doi.org/10.1016/j.ijleo.2020.164342.
23. Muzakkar, M.Z.; Umar, A.A.; Ilham, I.; Saputra, Z.; Zulfikar, L. Chalcogenide material as high

photoelectrochemical performance Se doped TiO_2/Ti electrode: Its application for Rhodamine B degradation. *J. Phys. Conf. Ser.* **2019**, *1242*, 1–8, https://doi.org/10.1088/1742-6596/1242/1/012016.

24. Paolini, R.; Borroni, D.; Pedeferri, M.; Diamanti, M.V. Self-cleaning building materials: The multifaceted effects of titanium dioxide. *Constr. Build. Mater.* **2018**, *182*, 126–133, https://doi.org/10.1016/j.conbuildmat.2018.06.047.
25. Santhana, V.; Thangaraju, D.; Tanaka, A.; Inami, W.; JayaKumar, S.; Matsuda, S. Development of Hybrid TiO_2/Paint Sludge Extracted Microbe Composite for Enhanced Photocatalytic Dye Degradation. *J. Inorg. Organomet. Polym. Mater.* **2020**, *30*, 2805-2813, https://doi.org/10.1007/s10904-020-01448-2.
26. Basavarajappa, P.S.; Patil, S.B.; Ganganagappa, N.; Reddy, K.R.; Raghu, A. V; Reddy, C.V. Recent progress in metal-doped TiO_2, non-metal doped/co-doped TiO2 and TiO2 nanostructured hybrids for enhanced photocatalysis. *Int. J. Hydrogen Energy* **2020**, *45*, 7764–7778, https://doi.org/10.1016/j.ijhydene.2019.07.241.
27. Lin, H.; Shih, C. Efficient one-pot microwave-assisted hydrothermal synthesis of M (M= Cr, Ni, Cu, Nb) and nitrogen co-doped TiO_2 for hydrogen production by photocatalytic water splitting. *J. Mol. Catal. A Chem.* **2016**, *411*, 128–137, https://doi.org/10.1016/j.molcata.2015.10.026.
28. Sharotri, N.; Sharma, D.; Sud, D. Experimental and theoretical investigations of Mn-N-co-doped TiO_2 photocatalyst for visible light induced degradation of organic pollutants. *J. Mater. Res. Technol.* **2019**, https://doi.org/10.1016/j.jmrt.2019.07.008.
29. Pan, L.; Xu, G.; Guo, T.; Zhang, B.; Xiang, S.; Fang, G.; Li, J. Study on thermochromic-emissivity performance of Mn doped TiO_2 under temperature fluctuations. *Infrared Phys. Technol.* **2020**, https://doi.org/10.1016/j.infrared.2020.103192.
30. Habibi, S.; Jamshidi, M. Sol–gel synthesis of carbon-doped TiO_2 nanoparticles based on microcrystalline cellulose for efficient photocatalytic degradation of methylene blue under visible light. *Environ. Technol. (United Kingdom)* **2020**, 3233-3247, https://doi.org/10.1080/09593330.2019.1604815.
31. Bento, R.T.; Correa, O. V.; Pillis, M.F. On the surface chemistry and the reuse of sulfur-doped TiO_2 films as photocatalysts. *Mater. Chem. Phys.* **2021**, *261*, 124231, https://doi.org/10.1016/j.matchemphys.2021.124231.
32. Du, M.; Qiu, B.; Zhu, Q.; Xing, M.; Zhang, J. Fluorine doped TiO_2/mesocellular foams with an efficient photocatalytic activity. *Catal. Today* **2019**, *327*, 340–346, https://doi.org/10.1016/j.cattod.2018.03.066.
33. Feng, X.; Wang, P.; Hou, J.; Qian, J.; Ao, Y.; Wang, C. Significantly enhanced visible light photocatalytic efficiency of phosphorus doped TiO_2 with surface oxygen vacancies for ciprofloxacin degradation: Synergistic effect and intermediates analysis. *J. Hazard. Mater.* **2018**, *351*, 196–205, https://doi.org/10.1016./j.jhazmat.2018.03.013.
34. Calisir, M.D.; Gungor, M.; Demir, A.; Kilic, A.; Khan, M.M. Nitrogen-doped TiO_2 fibers for visible-light-induced photocatalytic activities. *Ceram. Int.* **2020**, https://doi.org/10.1016/j.ceramint.2020.03.250.
35. Zeng, L.; Lu, Z.; Li, M.; Yang, J.; Song, W.; Zeng, D.; Xie, C. A modular calcination method to prepare modified N-doped TiO_2 nanoparticle with high photocatalytic activity. *Appl. Catal. B Environ.* **2016**, *183*, 308–316, https://doi.org/10.1016/j.apcatb.2015.10.048.
36. Burda, C.; Lou, Y.; Chen, X.; Samia, A.C.S.; Stout, J.; Gole, J.L. Enhanced nitrogen doping in TiO2 nanoparticles. *Nano Lett.* **2003**, *3*, 1049–1051, https://doi.org/10.1021/nl034332o.
37. Chong, M.N.; Tneu, Z.Y.; Poh, P.E.; Jin, B.; Aryal, R. Synthesis, characterisation and application of TiO_2–zeolite nanocomposites for the advanced treatment of industrial dye wastewater. *J. Taiwan Inst. Chem. Eng.* **2015**, *50*, 288–296, https://doi.org/10.1016/j.jtice.2014.12.013.
38. Mursalim, L.O.; Ruslan, A.M.; Safitri, R.A.; Azis, T.; Maulidiyah; Wibowo, D.; Nurdin, M. Synthesis and photoelectrocatalytic performance of Mn-N-TiO_2/Ti electrode for electrochemical sensor. *Proceedings of the IOP Conference Series: Materials Science and Engineering* **2017**, 267, https://doi.org/10.1088/1757-899X/267/1/012006
39. Nurdin, M.; Ramadhan, L.O.A.N.; Darmawati, D.; Maulidiyah, M.; Wibowo, D. Synthesis of Ni, N co-doped TiO_2 using microwave-assisted method for sodium lauryl sulfate degradation by photocatalyst. *J. Coatings Technol. Res.* **2017**, *15*, 395–402, https://doi.org/10.1007/s11998-017-9976-8.
40. Nurdin, M.; Muzakkar, M.Z.; Maulidiyah, M.; Maulidiyah, N.; Wibowo, D. Plasmonic Silver—N/TiO_2 Effect on Photoelectrocatalytic Oxidation Reaction. *J. Mater. Environ. Sci* **2016**, *7*, 3334–3343.
41. Maulidiyah, M.; Azis, T.; Lindayani, L.; Wibowo, D.; Salim, L.O.A.; Aladin, A.; Nurdin, M. Sol-gel TiO_2/Carbon Paste Electrode Nanocomposites for Electrochemical-assisted Sensing of Fipronil Pesticide. *J. Electrochem. Sci. Technol.* **2019**, *10*, 394–401, https://doi.org/10.33961/jecst.2019.00178.
42. Peng, T.; Ray, S.; Veeravalli, S.S.; Lalman, J.A.; Arefi-Khonsari, F. The role of hydrothermal conditions in determining 1D TiO_2 nanomaterials bandgap energies and crystal phases. *Mater. Res. Bull.* **2018**, *105*, 104–113, https://doi.org/10.1016/j.materresbull.2018.04.021.
43. Nurdin, M.; Zaeni, A.; Rammang, E.T.; Maulidiyah, M.; Wibowo, D. Reactor design development of chemical oxygen demand flow system and its application. *Anal. Bioanal. Electrochem.* **2017**, *9*, 480-494.
44. Zhang, Q.; Wang, H.; Fan, X.; Lv, F.; Chen, S.; Quan, X. Fabrication of TiO_2 nanofiber membranes by a simple dip-coating technique for water treatment. *Surf. Coatings Technol.* **2016**, https://doi.org/10.1016/j.surfcoat.2016.04.054.
45. Gurkan, Y.Y.; Turkten, N.; Hatipoglu, A.; Cinar, Z. Photocatalytic degradation of cefazolin over N-doped

TiO_2 under UV and sunlight irradiation: Prediction of the reaction paths via conceptual DFT. *Chem. Eng. J.* **2012**, *184*, 113–124, https://doi.org/10.1016/j.cej.2012.01.011.

46. Choudhury, B.; Borah, B.; Choudhury, A. Extending photocatalytic activity of TiO_2 nanoparticles to visible region of illumination by doping of cerium. *Photochem. Photobiol.* **2012**, *88*, 257–264, https://doi.org/10.1111/j.1751-1097.2011.01064.x.